CHEMISTRY OF MATERIALS

Subscriber access provided by University of South Dakota

Article

Construction of Efficient Deep Blue AIE Luminogen from Triphenylethylene for Non-Doped OLED Applications

Wei Qin, Zhiyong Yang, Yibin Jiang, Jacky W.Y. Lam, Guodong Liang, Hoi Sing Kwok, and Ben Zhong Tang

Chem. Mater., **Just Accepted Manuscript** • DOI: 10.1021/acs.chemmater.5b00568 • Publication Date (Web): 05 May 2015

Downloaded from http://pubs.acs.org on May 8, 2015

Just Accepted

"Just Accepted" manuscripts have been peer-reviewed and accepted for publication. They are posted online prior to technical editing, formatting for publication and author proofing. The American Chemical Society provides "Just Accepted" as a free service to the research community to expedite the dissemination of scientific material as soon as possible after acceptance. "Just Accepted" manuscripts appear in full in PDF format accompanied by an HTML abstract. "Just Accepted" manuscripts have been fully peer reviewed, but should not be considered the official version of record. They are accessible to all readers and citable by the Digital Object Identifier (DOI®). "Just Accepted" is an optional service offered to authors. Therefore, the "Just Accepted" Web site may not include all articles that will be published in the journal. After a manuscript is technically edited and formatted, it will be removed from the "Just Accepted" Web site and published as an ASAP article. Note that technical editing may introduce minor changes to the manuscript text and/or graphics which could affect content, and all legal disclaimers and ethical guidelines that apply to the journal pertain. ACS cannot be held responsible for errors or consequences arising from the use of information contained in these "Just Accepted" manuscripts.

ACS Publications
High quality. High impact.

Chemistry of Materials is published by the American Chemical Society. 1155 Sixteenth Street N.W., Washington, DC 20036

Published by American Chemical Society. Copyright © American Chemical Society. However, no copyright claim is made to original U.S. Government works, or works produced by employees of any Commonwealth realm Crown government in the course of their duties.

Construction of Efficient Deep Blue AIE Luminogen from Triphenylethene for Non-Doped OLED Applications

Wei Qin,[†,‡,⊥] Zhiyong Yang,[†,‡,⊥] Yibin Jiang,[§] Jacky W. Y. Lam,[†,‡] Guodong Liang,[†,‡] Hoi Sing Kwok,[§] and Ben Zhong Tang[†,‡,#,*]

[†]HKUST-Shenzhen Research Institute, No. 9 Yuexing 1st RD, South Area, Hi-tech Park, Nanshan, Shenzhen, 518057, China

[‡]Department of Chemistry, Institute for Advanced Study, Division of Life Science, State Key Laboratory of Molecular Neuroscience, Institute of Molecular Functional Materials and Division of Biomedical Engineering, The Hong Kong University of Science & Technology, Clear Water Bay, Kowloon, Hong Kong, China

[§]Center for Display Research, HKUST, Clear Water Bay, Kowloon, Hong Kong, China

[#]Guangdong Innovative Research Team, SCUT-HKUST Joint Research Laboratory, State Key Laboratory of Luminescent Materials and Device, South China University of Technology, Guangzhou, 510640, China

---

ABSTRACT: Deep blue emitters are crucial for full color displays and organic white lighting. Thanks to the research efforts by scientists, many efficient light emitters with aggregation-induced emission (AIE) characteristics have been synthesized and found promising applications in organic light-emitting devices (OLEDs). However, few AIE emitters with deep blue emissions and excellent electroluminescence (EL) performance have been reported. The contribution here reports a simple but successful molecular design strategy for synthesizing efficient solid-state emitters for non-doped OLEDs with both deep blue and white emissions. This strategy utilizes triphenylethene, a weakly conjugated AIEgen as building block for constructing deep blue emitter, involving no complicated control on emission color through adjustment of the steric hindrance of chromohphores and enables a wide selection of partnered functional units. The synthesized AIE luminogen, abbreviated as BTPE-PI, is thermally stable and exhibits high fluorescence quantum efficiency as well as good charge injection capability in the solid state. Non-doped deep blue OLED fabricated from BTPE-PI shows a very high external quantum efficiency of 4.4% with a small roll-off, whose performance is the best among deep blue AIE materials reported so far. An efficient white OLED with Commission Internationale de l'Eclairage (CIE) coordinates of (0.33, 0.33) at theoretical white point was first achieved by using AIE luminogen BTPE-PI as deep blue emitter. Such molecular design strategy opens a new avenue in the development of efficient solid-state deep blue emitters for non-doped OLED applications.

INTRODUCTION

Development of efficient luminescent materials with primary RGB (red, green and blue) colors in the solid state is critical for the applications in organic light-emitting diodes (OLEDs).[1] Among the primary RGB colors, deep blue emission is important for full color displays and organic white lighting.[2,3] It can also offer a wide-gamut RGB color space, which possesses high saturated and "pure" light colors.[4] On the other hand, it can be used as an excitation source to activate other color emissions through energy transfer.[5] However, luminophores with efficient deep blue emission are rare. Despite of their high external quantum efficiency in electroluminescence (EL) devices, organometallic complexes with deep blue emissions are rarely observed because of the consumption of the energy of the high level metal-ligand charge transfer bond by the metal *d* orbitals through non-radiative relaxation channel.[6–8] Therefore, considerable attentions have been placed on fluorophores with this emission color. Even such emitters are prepared, it is challenging to utilize them for fabricating OLEDs with good performance as their wide band-gaps[9] tend to create large charge injection barrier and unbalanced charge injection and transportation, leading to increased driving voltage and lowered device efficiency.[10] On the other hand, a problem associated with most blue luminogenic materials is the aggregation-caused quenching (ACQ) of light emission in the aggregated state: their intense emission in the solution state is weakened[11] and red-shifted to undesirable sky blue color when their molecules are aggregated[12] due to the severe intermolecular interaction.[13,14]

Several strategies have been adopted to solve the abovementioned problems. To improve the charge balance in OLEDs and hence enhance the EL efficiency, introduction of donor (D) and acceptor (A) units into the luminogenic structure[15,16] has been proved to be effective method because of the creation of the intramolecular charge transfer (ICT) effect. However, the extent of ICT effect should be well controlled as strong D-A pair tends to induce excessive bathochromic shift and normally impairs the emission color purity.[17] On the other side, to mitigate the ACQ effect, methods of cross dipole stacking,[18] *J*-aggregate formation[19,20] and introduction of bulky substituents[11,21–24] have been employed. However, these methods are far from satisfactory. For example, to achieve a particular stacking mode, careful molecular design and control on the luminogen aggregation are required. Integration of bulky alkyl groups[25–27] is often accompanied with severe side effects, such as dilution of chromophore concentration and obstruction of the charge injection and transportation in EL devices.

We observed a phenomenon of aggregation-induced emission (AIE) in some organic luminophores with twisted conformations.[12,28–30] These molecules are non-emissive in dilute solutions because of their active intramolecular motions, which consume the energy of the excitons through non-radiative relaxation pathways. Such motions, however, are restricted in the aggregated state, which enables the excitons to decay radiatively. The twisted conformations of the molecules also prevent the formation of detrimental species such as exciplexes and excimers by strong intermolecular interactions. All these factors make the AIE luminogens to show strong light emission in the aggregated state. Integration of AIE units to conventional ACQ chromophores has been found to be a good strategy to solve their ACQ problem and generates new luminogens with high fluorescence quantum efficiencies and inherited properties from both the parent molecules.[31,32] Such design strategy thus offers a formulated platform to generate functional luminescent materials with efficient solid-state emissions.

Limited by the long conjugation length of some typical AIE luminogens such as tertraphenylethene and silole,[33,34] it is difficult to achieve deep blue emission when using them as building blocks. Few such emitters have been prepared but their design involves complicated control on their steric hindrance.[35,36] On the other hand, as these emitters generally possess highly twisted structures, their EL performances are only moderate due to the poor charge transportation. Thus, a simple and direct method to tackle the above problem is to find an AIE luminogen with efficient emission but low conjugation. With such AIE unit, complicated design and synthesis of luminogens with highly twisted structures or severe steric hindrance are not needed and meanwhile a much wider partnered functional units can be selected for luminogen construction. Following this idea, triphenylethene (TPE) is selected as the main molecular skeleton. Although it possesses a low conjugation, it and its derivatives show splendid AIE characteristics.[37,38] Compared to tetraphenylethene in the solid state, its emission is much bluer, exhibiting a hypsochromatic shift in the emission maximum of as large as 25 nm (Figure S1 in the Supporting Information). Such property should significantly improve the color purity of its derivatives. On the other side, we utilized phenanthro[9,10-d]imidazole (PI) as a deep blue building block for its good thermal and carrier injection properties.[39,40] Last, covalent combination of these two parts produce a luminogen, where one TPE moiety (A) is connected to the phenyl ring of PI at the *para* position to impart good conjugation and hence improved charge transportation.[41] The another TPE unit (B) is linked laterally at the *meta* position to lower the conjugation and hence shorten the emission wavelength (Chart 1). This also endows the molecule a twisted conformation, which can prevent undesirable intermolecular interactions in the solid state.

In this paper, we demonstrate a new molecular design strategy and report the synthesis of an efficient deep blue AIE luminogen constructed from triphenylethene and PI. The synthesized luminogen, abbreviated as BTPE-PI, is thermally stable with balanced carrier injection properties. Non-doped multilayer EL devices fabricated by using BTPE-PI as emitting layer, showed deep blue EL with external quantum efficiency of as high as 4.4% and a small roll-off. In addition, efficient white EL device with Commission Internationale de l'Eclairage (CIE) coordinates of (0.33, 0.33) at the exact theoretical white point was first achieved by employing AIE luminogen (BTPE-PI) as the blue deep emitter. Such good results indicated that such strategy on molecular design shed some light on the development of efficient deep blue luminescent materials for OLED applications.

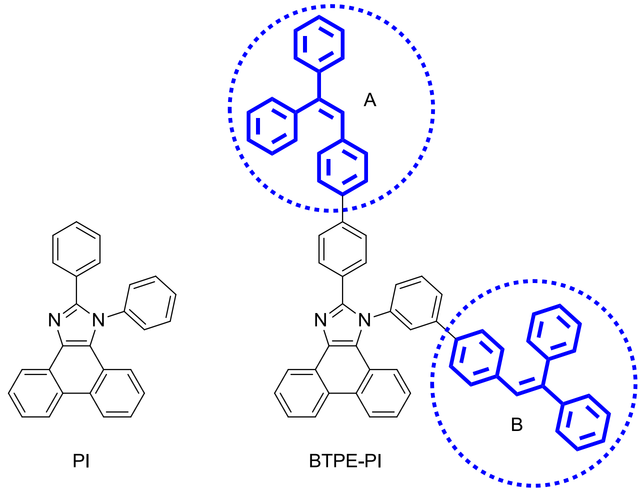

Chart 1. Chemical structures of PI and BTPE-PI.

EXPERIMENTAL SECTION

Materials. THF was distilled from sodium benzophenone ketyl under dry nitrogen immediately prior to use. Intermediates **5**[42], **6**[43], **7**[44] and tetraphenylethene[45] were prepared according to the reported experimental procedures. Other chemicals and reagents were purchased from Aldrich and used as received without further purification.

Characterization. ^{1}H and ^{13}C NMR spectra were measured on a Bruker AV 400 spectrometer in CD_2Cl_2 or $CDCl_3$ using tetramethylsilane (TMS; δ = 0) as internal reference. High resolution mass spectra (HRMS) were recorded on a GCT premier CAB048 mass spectrometer operating in MALDI-TOF mode. Elemental analysis was operated on a ThermoFinnigan Flash EA1112 analyzer. UV spectra were measured on a Milton Roy 5 Spectronic 3000 Array spectrophotometer. Photoluminescence spectra were recorded on a Perkin-Elmer LS 55 spectrofluorometer. The solution fluorescence quantum yields were determined by using 9,10-diphenylanthracene as standard (Φ_F = 90% in cyclohexane). The absorbance of the solutions was kept below 0.1 to avoid the internal filter effect. The emission efficiencies of thin films of PI and BTPE-PI were measured on a calibrated integrating sphere. Their thermal stabilities were measured on TGA Q5000 and DSC Q1000 instruments under nitrogen at a heating rate of 20 °C/min. Cyclic voltammetry (CV) experiments were carried out in dichloromethane solution with 0.1 M tetrabutylammonium hexafluorophosphate as the supporting electrolyte at a scan rate of 100 mV/s, by using Ag/$AgNO_3$ as the working electrode and saturated calomel electrode (SCE) as the reference electrode.

Synthesis. *Preparation of PI*: The compound was prepared according to the reported methods[46] with a slight modification. Into a stirred mixture of 9,10-phenanthrenequinone (624 mg, 3 mmol), benzaldehyde (318 mg, 3 mmol), aniline (1.4 g, 15 mmol) and ammonium acetate (2.87 g, 37.2 mmol), 20 mL of glacial acetic acid was added under nitrogen. The mixture was heated to reflux for 12 h. After cooling to room temperature, a pale yellow mixture was obtained and poured into a methanol solution under stirring. The precipitates were filtered, washed with methanol, and dried to give a pale yellow solid. After filtration and solvent evaporation under reduced pressure, the product was purified by silica-gel column chromatography using hexane/dichloromethane as eluent. It was further purified by stirring in reflux ethanol. After subsequent filtration and drying in vacuum, PI was obtained in 53.2% yield (591 mg) as a white powder. ^{1}H NMR (400 MHz, CD_2Cl_2, δ): 8.79 (t, J = 8.0 Hz, 2H), 8.74 (d, J = 8.4 Hz, 1H), 7.85–7.83 (m, 1H), 7.76 (td, J = 8.0, 0.8 Hz, 1H), 7.72–7.67 (m, 2H), 7.59–7.46 (m, 7H), 7.35 (td, J = 8.0, 0.8 Hz, 1H), 7.22 (d, J = 8.4 Hz, 1H). ^{13}C NMR (100 MHz, CD_2Cl_2, δ): 150.01, 140.19, 137.80, 133.75, 132.45, 131.97, 131.91, 131.21, 129.72, 129.64, 128.69, 128.62, 128.39, 127.83, 127.45, 126.98, 126.22, 125.62, 124.59, 123.89, 123.84, 123.62, 123.13, 122.89, 121.19. HRMS (MALDI-TOF), m/z: M$^+$, calcd. for $C_{27}H_{18}N_2$, 370.1470; found, 370.1479.

Preparation of BBr-PI: The compound was prepared from 9,10-phenanthrenequinone (624 mg, 3 mmol), 4-bromobenzaldehyde (555 mg, 3 mmol), 3-bromoaniline (2.58 g, 15 mmol, 1.65 mL), ammonium acetate (2.87 g, 37.2 mmol) and 20 mL of glacial acetic acid by following the same procedure described above, affording a white solid in 51.0% yield (808 mg). ^{1}H NMR (400 MHz, CD_2Cl_2, δ): 8.79 (t, J = 8.0 Hz, 2H), 8.74 (d, J = 8.4 Hz, 1H), 7.85–7.83 (m, 1H), 7.76 (td, J = 8.0, 0.8 Hz, 1H), 7.72–7.67 (m, 2H), 7.59–7.46 (m, 7H), 7.35 (td, J = 8.0, 0.8 Hz, 1H), 7.22 (d, J = 8.4 Hz, 1H). ^{13}C NMR (100 MHz, CD_2Cl_2, δ): 150.01, 140.19, 137.80, 133.75, 132.45, 131.97, 131.91, 131.21, 129.72, 129.64, 128.69, 128.62, 128.39, 127.83, 127.45, 126.98, 126.22, 125.62, 124.59, 123.89, 123.84, 123.62, 123.13, 122.89, 121.19. HRMS (MALDI-TOF), m/z: M$^+$, calcd. for $C_{27}H_{16}Br_2N_2$, 527.9660; found, 527.9673.

Preparation of BTPE-PI: Into a stirred mixture of BBr-PI (264 mg, 0.5 mmol), 4-(2,2-diphenylvinyl)phenylboronic acid (600 mg, 2.0 mmol), $Pd(PPh_3)_4$ (57 mg) and K_2CO_3 (1.24 g, 9 mmol), 40 mL of THF and 5 mL of water was added under nitrogen. The mixture was heated to 70 °C for 24 h. After cooling to room temperature, the solution was extracted with dichloromethane (150 mL × 2), washed with water and dried over Na_2SO_4. After filtration and solvent evaporation under reduced pressure, the product was purified by silica-gel column chromatography using hexane/dichloromethane as eluent. BTPE-PI was obtained in 54% yield (237 mg) as a white powder. ^{1}H NMR (400 MHz, CD_2Cl_2, δ): 8.82–8.78 (m, 2H), 8.73 (d, J = 8.4 Hz, 1H), 7.86 (dd, J = 8.0, 1.2 Hz, 1H), 7.77–7.74 (m, 2H), 7.69–7.65 (m, 4H), 7.54–7.49 (m, 4H), 7.40–7.27 (m, 22H), 7.24–7.21 (m, 2H), 7.20–7.17 (m, 2H), 7.10–7.06 (m, 4H), 7.02 (s, 1H), 7.0 (s, 1H). ^{13}C NMR (100 MHz, CD_2Cl_2, δ): 150.81, 143.70, 143.56, 143.35, 143.04, 140.92, 140.83, 140.70, 139.71, 138.45, 137.89, 137.81, 137.62, 137.36, 130.99, 130.67, 130.60, 130.51, 130.41, 129.99, 129.87, 129.49, 129.14, 128.69, 128.60, 128.42, 128.02, 127.93, 127.89, 127.70, 127.61, 127.50, 126.88, 126.83, 126.75, 126.69, 125.97, 125.31, 124.49, 123.60, 123.47, 122.90, 121.33. HRMS (MALDI-TOF), m/z: M$^+$, calcd. for $C_{67}H_{46}N_2$, 878.3661; found, 878.3678. Anal. calcd (%) for $C_{67}H_{46}N_2$: C 91.54, H 5.27, N 3.19; found: C 91.44, H 5.37, N, 3.20.

Preparation of nanoaggregates. Stock THF solutions of PI and BTPE-PI were prepared with a concentration of 10^{-4} M. Aliquots of the stock solutions were transferred to 10 mL volumetric flasks. After appropriate amounts of THF were added, water was added dropwise under vigorous stirring to prepare 10^{-5} M solutions with different water contents (0–90 vol %). The PL spectra of the resultant solutions were immediately measured.

Device fabrication. The devices were fabricated on 80 nm ITO-coated glass with a sheet resistance of 25 Ω per square. Before loading into the pretreatment chamber, the ITO-coated glasses were soaked in ultrasonic detergent for 0.5 h, followed by spraying with deionized water for 10 min, soaking in ultrasonic deionized water for 0.5 h, and oven-baking for 1 h. The cleaned samples were treated by fluoroform (CHF_3) plasma with a power of 10 W, gas flow of 50 sccm, and pressure of 0.2 Torr for 10 s in the pretreatment chamber. The solid samples were transferred to the organic chamber with a base pressure of 5×10^{-7} Torr for the deposition of NPB, BTPE-PI and TPBi. The samples were then transferred to the metal chamber for the deposition of cathode, which was composed of lithium fluoride (LiF) capped with aluminium (Al). The light-emitting area was 4 mm^2 as defined by the overlap of the cathode and anode. The current density–voltage-luminance characteristic curves of the devices were determined by a HP4145B semiconductor parameter analyzer and a calibrated UDT PIN-25D silicon photodiode. The luminance and external quantum efficiencies of the devices were inferred from the photocurrent of the photodiode. The EL spectra were measured by a PR650 spectrophotometer. All the measurements were performed at room temperature under air without device encapsulation.

RESULTS AND DISCUSSION

Synthesis and Characterization. BTPE-PI and PI were prepared facilely according to the synthetic routes shown in Scheme S1. The key intermediate BBr-PI was prepared from 9,10-phenanthrenequinone (**1**) according to previously published synthetic procedures.[46] BTPE-PI was obtained by Suzuki coupling of BBr-PI and 4-(2,2-diphenylvinyl)phenylboronic acid (**7**) using $Pd(PPh_3)_4$ as a catalyst under basic conditions. All the intermediates and product were characterized by standard spectroscopic techniques, which gave satisfactory analysis data corresponding to their chemical structures and demonstrated their high purity. Detailed synthetic procedures and examples of ^1H NMR and mass spectra were shown in Figures S2 and S3.

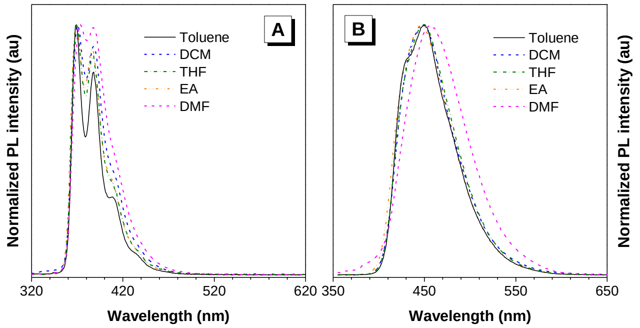

Figure 1. Normalized PL spectra of (A) PI and (B) BTPE-PI in different solvents. Excitation wavelength (nm): 312 (PI) and 340 (BTPE-PI).

Optical properties. BTPE-PI possesses a good solubility in common organic solvents, such as dichloromethane, chloroform and tetrahydrofuran (THF), but is insoluble in water. The UV spectra of PI and BTPE-PI measured in THF are peaked at 312 and 340 nm, respectively (Figure S4). The associated molar absorptivity (7.2×10^4 L mol^{-1} cm^{-1}) for BTPE-PI is 3-fold higher than that of PI due to its more conjugated structure. In THF solution, PI emits a strong purple photoluminescence (PL) at 370 and 387 nm, while the PL spectrum of BTPE-PI was centered in the blue region at ~449 nm. The PL spectra of PI and BTPE-PI measured in different solvents are shown in Figure 1. When the solvent is changed from nonpolar toluene to polar *N*,*N*-dimethylformamide, the emission maximum red-shifts but in a small extent (~4 nm for PI and ~6 nm for BTPE-PI). Under similar conditions, the emission of 4-(*N*,*N*-dimethylamino)benzonitrile, a typical strong D-A molecule, shifts bathochromically by ~100 nm.[47] This suggests that both PI and BTPE-PI are insensitive to solvent polarity and show a weak D-A interaction, which is beneficial for the improvement of charge balance in OLEDs but will not cause excessive emission red-shift. Their PL properties are also studied in THF/water mixtures with different water fractions (f_w) with a view to study the effects of solvent polarity and aggregation on their light emission process. When a small amount of water (f_w <70 vol %) was added to the THF solution of PI, its PL intensity was enhanced slightly. Further increment of the water content, however, weakens the light emission. At f_w = 90%, the PL intensity is merely 50% of that in pure THF solution (Figures 2A and 2B). Since PI is insoluble in water, its molecules should form aggregates in solvent mixtures with high water contents. Clearly, like most conventional chromophores, the PL of PI is quenched by aggregate formation. Similar phenomenon was also observed upon solution thickening. The emission was significantly quenched when the solution concentration was increased from 10 μM to 1 mM (Figure S5). On the other hand, attachment of TPE units to PI has endowed the resulting adduct (BTPE-PI) with AIE attribute. As shown in Figures 2C and 2D, the peak intensity of BTPE-PI was slightly weakened upon addition of a small amount of water (f_w ≤ 50 vol %). Afterwards, the emission becomes stronger swiftly. The maximum emission enhancement was observed at f_w = 90%, being ~5-fold higher than that in pure THF solution. Evidently, BTPE-PI is AIE-active. Quantitative measurements on their fluorescence quantum yields (Φ_F) in solution and solid states also draw the same conclusion. The Φ_F of PI in pure THF solution is 58.8%, which drops to 38.2% in the thin film state accompanied with a ~30 nm red-shift in emission because of strong intermolecular interactions (Table 1). In contrast, the thin film of BTPE-PI emits at a spectral region similar to that in the solution state but exhibits a much higher Φ_F (93.8% *vs* 14.5%). Thus, this highly blue emissive luminogen is a promising candidate for the fabrication of efficient EL device.

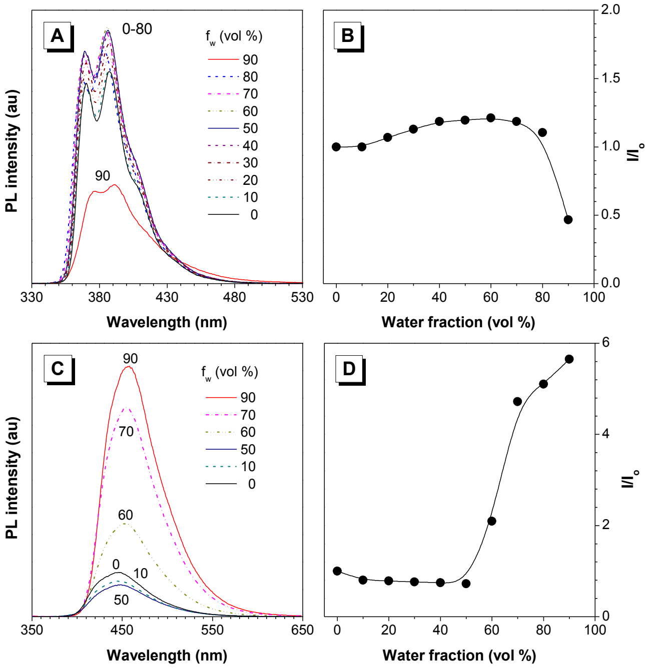

Figure 2. PL spectra of (A) PI and (C) BTPE-PI in THF/water mixtures with different water fractions (f_w). Plots of relative PL intensity (I/I_o) versus the composition of THF/water mixtures of (B) PI and (D) BTPE-PI. I_o = emission intensity in pure THF solution. Concentration: 10 μM; excitation wavelength (nm): 312 (PI) and 340 (BTPE-PI).

Electronic properties. To get a further insight into the photophysical properties of PI and BTPE-PI at the molecular level, density functional theory calculations are carried out using a suite of Gaussian 03 program. The nonlocal density functional of B3LYP with 6-31G (d) basis sets was used for the calculation. The highest occupied molecular orbital (HOMO) of BTPE-PI was dominated by the orbitals from the PI core and TPE (A) unit on the same axis. The electron cloud of the lowest unoccupied molecular orbital (LUMO), however, was located mainly on the PI core and the lateral TPE (B) unit (Figure S6). Such electron distribution imparts BTPE-PI an intrinsic intramolecular charge transfer property. The dipole moment of BTPE-PI is small and equal to 5.29, which is indicative of a weak D-A property and is consistent with the experimental data given in Figure 1. The optimized structures of PI and BTPE-PI are shown in Figure S7 for comparison. PI adopts an almost planar conformation, which favors strong intermolecular interactions that lead to fluorescence quenching. On the contrary, BTPE-PI is non-planar. The torsion angles between the imidazole plane (a) and the adjacent phenyl rings are 18.6° (phenyl ring b) and 88.9° (phenyl ring f). In such case, the PI core is well-conjugated with the TPE (A) unit that lies on the same axis but shows a poor electronic communication with the lateral one (B). The dihedral angles between the PI unit and the TPE moieties are both ~35°, while those between any phenyl ring and the olefin core of the TPE unit fall in the range from 22.7° to 64.9° (Table S1). The non-planar conformation of BTPE-PI is mainly attributed to the propeller-shaped TPE units, which disfavor the close molecular packing in the solid state. Coupled with the restriction of intramolecular motions in the aggregated state, all these made BTPE-PI an efficient solid-state emitter.

Thermal properties. The thermal properties of PI and BTPE-PI are examined by thermogravimetric analysis (TGA) and differential scanning calorimetry (DSC) measurements (Figure 3 and Table 1). BTPE-PI is thermally very stable, exhibiting a 5% weight loss at 460 °C. Such value is much higher than that of PI (T_d = 262 °C) (Figure 3A). The glass transition temperature (T_g) of BTPE-PI was detected at 145 °C, while such thermal transition was not detected in PI (Figure 3B). No transition peak associated with crystallization was observed when BTPE-PI was heated up to 200 °C. The non-planar TPE units in BTPE-PI hinder close packing, thus making the luminogen non-crystalline or amorphous in nature. Luminogens with high thermal and morphological stabilities are beneficial for the formation of amorphous thin films by vacuum deposition, which is important for the stability of OLEDs.[48]

Electrochemical properties. The electrochemical properties as well as energy levels of BTPE-PI and PI are investigated by cyclic voltammetry (Figure S8 and Table 1). The HOMO of BTPE-PI is estimated from its oxidation onset potential and is calculated to be –5.50 eV. This suggests a good hole injection property due to the fine contribution from the PI unit (E_{HOMO} = –5.48 eV). Its LUMO can be obtained by addition of the optical band gap energy (E_g) estimated from the onset absorption wavelength from the HOMO value and is calculated to be –2.45 eV. This value is lower than that of PI (–2.16 eV) but close to that of 1,3,5-tri(phenyl-2-benzimidazolyl)-benzene (TPBi, –2.7 eV), which is widely used as an electron-injection layer in OLEDs.[49] Clearly, the electron injection ability of BTPE-PI is similar to TPBi but better than PI. This also suggests a good carrier injection property in BTPE-PI due to its suitable HOMO and LUMO energy levels. This property will enable the fabrication of devices with simple configurations, which is an advantage for practical OLED applications.

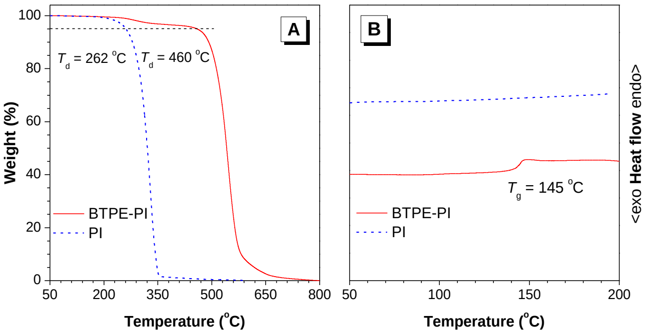

Figure 3. (A) TGA and (B) DSC (second heating cycle) thermograms of PI and BTPE-PI recorded under nitrogen at a heating rate of 20° C/min.

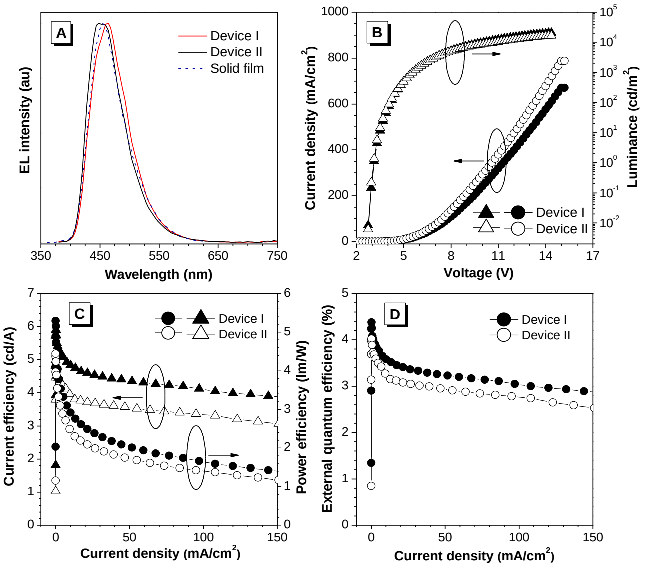

Figure 4. (A) PL and EL spectra of solid thin film of BTPE-PI. (B) Current density–voltage–luminance characteristics of multilayer EL devices of BTPE-PI. Changes in (C) current efficiency and power efficiency and (D) external quantum efficiency with the applied current density in multilayer EL devices of BTPE-PI. Device configuration: ITO/NPB/BTPE-PI/TPBi/LiF/Al.

Table 1. Optical and thermal properties of PI and BTPE-PI[a)]

Compound	λ_{ab} [nm]	E_{HOMO} [eV]	E_{LUMO} [eV]	E_g [eV]	λ_{em} [nm] soln ($\Phi_{F,s}$)	aggr	film ($\Phi_{F,f}$)	T_d/T_g [°C]
PI	312, 344, 362	−5.48	−2.16	3.32	370, 387 (58.8)	376, 391	397, 415 (38.2)	262/nd
BTPE-PI	340	−5.50	−2.45	3.05	449 (14.5)	456	455 (93.8)	460/145

[a)] Abbreviation: λ_{ab} = absorption maximum in THF, E_{HOMO} = highest occupied molecular orbitals calculated from the onset oxidation potential, E_g = energy band gap calculated from the onset of the absorption spectrum, E_{LUMO} = lowest unoccupied molecular orbitals estimated by using the equation: $E_{LUMO} = E_{HOMO} + E_g$, λ_{em} = emission maximum in THF solution (soln), THF/water mixture (1:9 by volume) (aggr) and solid thin film spin-coated from THF solution with fluorescence quantum yield (Φ_F) given in the parentheses, T_d = temperature for 5% weight loss, T_g = glass transition temperature, nd = not detected.

Table 2. EL performances of BTPE-PI[a)]

Device	λ_{EL} [nm]	V_{on} [V]	L_{max} [cd/m²]	$\eta_{C,max}$ [cd/A]	$\eta_{P,max}$ [lm/W]	$\eta_{ext,max}$ [%]	CIE (x, y)
I	463	3.2	20300	5.9 (4.6)	5.3 (2.5)	4.4 (3.4)	0.15, 0.15
II	450	3.2	16400	4.9 (3.7)	4.4 (3.1)	4.0 (3.0)	0.15, 0.12
III	450, 511, 618, 674	3.2	19200	10.7 (9.8)	8.1 (5.3)	6.4 (5.9)	0.33, 0.33

[a)] Abbreviation: λ_{EL} = EL maximum, V_{on} = turn-on voltage at 1 cd/m², L_{max} = maximum luminance, $\eta_{P,max}$ = maximum power efficiency, $\eta_{C,max}$ = maximum current efficiency and $\eta_{ext,max}$ = maximum external quantum efficiency. The values in the parentheses are taken at a luminance of 1000 cd/m². CIE (x, y) = Commission Internationale de l'Eclairage chromaticity coordinates collected at 8 V. Device configuration: ITO/NPB(60 nm)/BTPE-PI(20 nm)/TPBi(40 nm)/LiF(1 nm)/Al(100 nm) (Device I), ITO/NPB(40 nm)/BTPE-PI(20 nm)/TPBi(40 nm)/LiF(1 nm)/Al(100 nm) (Device II) and ITO/NPB(40 nm)/Ir(btp)$_2$(acac)(6 wt %):CBP(10 nm)/Ir(ppy)$_3$(8 wt %):CBP(4 nm)/CBP(3 nm)/BTPE-PI(5 nm)/TPBi(40 nm)/LiF/Al (Device III).

Electroluminescence. *Non-doped deep blue OLED.* The efficient solid-state deep blue emission of BTPE-PI as well as its high thermal stability and suitable LUMO and HOMO levels prompts us to investigate its EL properties. Most deep blue EL devices reported previously involve the use of dopants. However, to achieve an optimized device performance, careful control on the dopant concentration is required.[50,51] On the other hand, performance degradation due to phase separation upon heating is also a problem encountered in these devices.[52−54] Nevertheless, AIE luminogens are free from the ACQ effect and thus require no dopant for EL device fabrication. With such regard, we thus fabricated a non-doped OLED device with a simple configuration of ITO/NPB(60 nm)/BTPE-PI(20 nm)/TPBi(40 nm)/LiF(1 nm)/Al(100 nm) (Device I). In this device, BTPE-PI works as blue emitting layer (EML), *N*,*N*′-di(1-naphthyl)-*N*,*N*′-diphenyl-(1,1′-biphenyl)-4,4′-diamine (NPB) functions as a hole-transporting layer (HTL) and TPBi serves as both electron-transporting (ETL) and hole-blocking layer. The EL spectrum of device I was peaked at 463 nm, whose patten resembles the PL spectrum of the solid thin film. This confirms that the EL is indeed from the emitting layer. The device turns on at a very low bias voltage of 3.2 V and emits brilliant blue light with maximum luminance (L_{max}) of 20300 cd/m², maximum current efficiency ($\eta_{C,max}$) and power efficiency ($\eta_{P,max}$) of 5.9 cd/A, 5.3 lm/W, respectively (Figure 4 and Table 2). The external quantum efficiency ($\eta_{ext,max}$) is determined to be 4.4%, which is rather high and close to the theoretical limit (5%) for fluorescent materials. Driven at 1000 cd/m², the device also performs well with high η_{ext} of 3.4%. In addition, the roll-off is small, which drops merely 14.4% when the device brightness is increased from 1000 cd/m² to 5000 cd/m². The CIE coordinates are calculated to be (0.149, 0.147), which fall in the deep blue region (y <0.15)[17, 55−57] (Figures 5A and 5D).

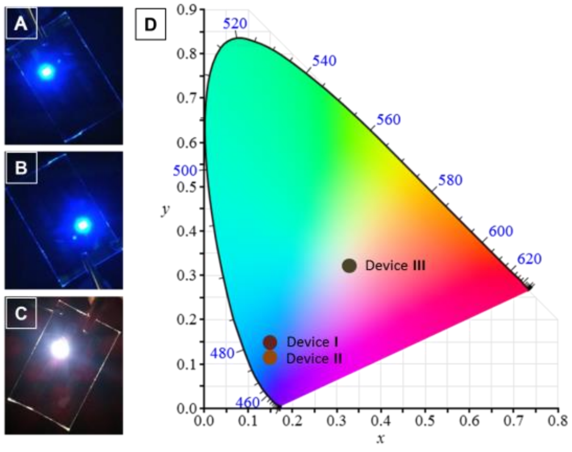

Figure 5. Photos of (A) Device I, (B) Device II and (C) Device III. (D) Commission Internationale de l'Eclairage (CIE) chromaticity coordinates of the three devices.

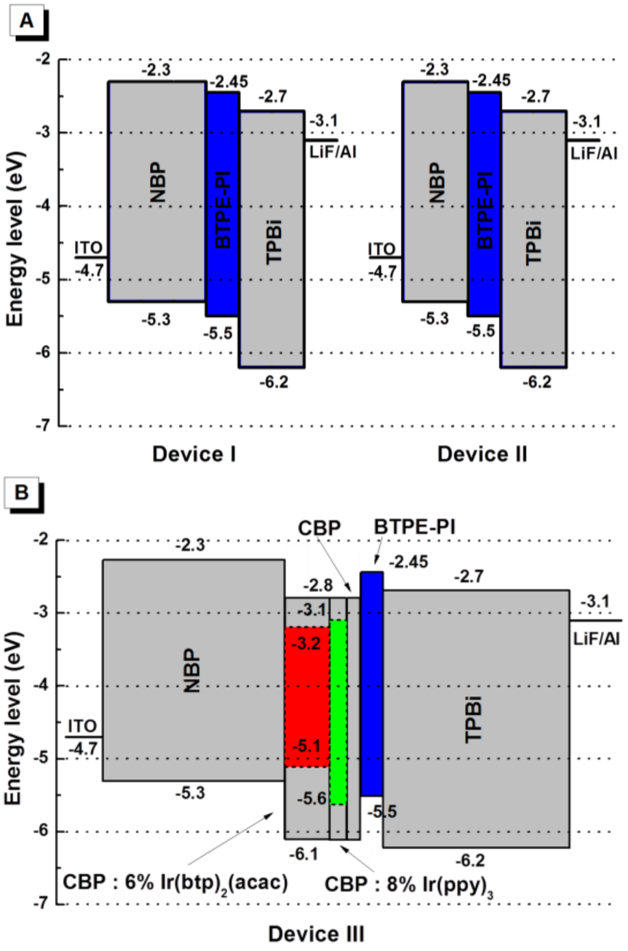

Figure 6. Energy level diagrams and device configurations of BTPE-PI based (A) deep blue (B) white OLEDs.

The excellent EL performance of BTPE-PI is somewhat related to its good charge injection property as well as its weak D-A system. To get a further insight, the energy level diagrams and device configurations of the EL devices are illustrated in Figure 6A. Thanks to the suitable energy levels of BTPE-PI, the electron injection barrier at the TPBi/BTPE-PI junction is only 0.25 eV, while the hole injection barrier is also small (0.20 eV) at the NPB/BTPE-PI junction. These small injection barriers enable efficient injection of both holes and electrons into the emitting layer at low bias. Moreover, the TPBi layer effectively blocks the leakage of holes from the emitting layer. These well matched energy levels are beneficial for charge balance and efficient exciton recombination at the emitting layer, thus improving the EL efficiency. By fine adjustment of the thickness of the hole-transporting layer, we can shift the EL spectrum to the shorter wavelength region due to the interference effect.[58–60] Device II with a configuration of ITO/NPB(40 nm)/BTPE-PI(20 nm)/TPBi(40 nm)/LiF(1 nm)/Al(100 nm) was also fabricated, which exhibits a bluer light than Device I with CIE coordinates of (0.15, 0.12) (Figures 5B, 5D and 6A). The device shows high performance with L_{max}, $\eta_{C,max}$, $\eta_{P,max}$ and $\eta_{ext,max}$ of 16400 cd/m^2, 4.9 cd/A, 4.4 lm/W and 4.0%, respectively (Table 2 and Figure 4). Table S2 compares the EL performances of BTPE-PI with those of deep blue emitters reported previously.[17,23,35,36,46,61–72] The EL devices fabricated from BTPE-PI with standard three-component active layers (HTL/EML/ETL) exhibit really high performance and energy conversion as reflected by their high external quantum and power efficiencies. The maximum luminance (> 15000 cd/m^2) attained by them are one order of magnitude higher than the previous results. Some EL devices with excellent $\eta_{ext,max}$ (>5%) have been reported[62,63,71,72] but their device structures are complicated and involve four-component active layers. When driven at 1000 cd/m^2 for practical applications, most of these devices show an obvious efficiency roll-off. The BTPE-PI based EL devices, however, still retain very high performances with efficiencies of up to 3.1% and 3.0 lm/W. Such results are impressive and are the best among the deep blue non-doped OLEDs.

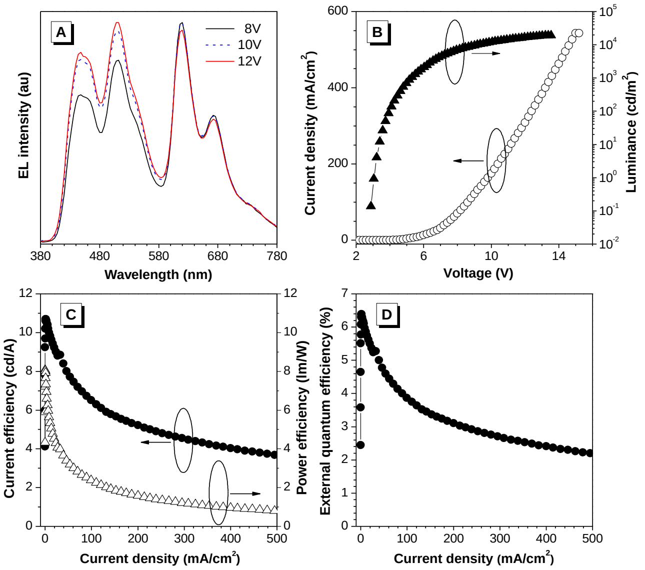

Figure 7. (A) EL spectra of a multilayer WOLED at different applied voltages. (B) Current efficiency–voltage–luminance characteristics of a multilayer WOLED. Changes in (C) current efficiency and power efficiency and (D) external quantum efficiency with the applied current density in a multilayer WOLED. Device configuration: ITO/NPB/Ir(btp)2(acac):CBP/Ir(ppy)3:CBP/CBP/BTPE-PI/TPBi/LiF/Al.

White light OLED. One of the most important applications for deep blue emitters is the fabrication of white OLED (WOLED).[73,74] Many WOLEDs containing primary RGB emitters were fabricated, showing unique advantages of high stability of blue fluorophores and high efficiency of phosphors with longer emission wavelength. Their multilayer structure allows flexible manipulation of each EML as well as the precise control on the exciton distribution in different EMLs. We fabricated a white EL device with a configuration of ITO/NPB(40 nm)/Ir(btp)$_2$(acac)(6 wt %):CBP(10 nm)/Ir(ppy)$_3$(8 wt %):CBP(4 nm)/mCP(3 nm)/BTPE-PI(5 nm)/TPBi(40 nm)/LiF/Al, where BTPE-PI functions as blue emitting layer, bis[2-(2'-benzothienyl)pyridinato-N,C3'](acetylacetonato)iridium(III) Ir(btp)$_2$(acac) and tris[2-phenylpyridinato-C2,N]iridium(III) Ir(ppy)$_3$ work as red and green emitters, respectively, and 4,4'-bis(9*H*-carbazol-9-yl)biphenyl CBP was used as host to reduce the structural heterogeneity and facilitate charge transport between the adjacent red and green emitting layers. A 3 nm thickness of 1,3-bis(carbazol-9-yl)benzene (mCP) buffer layer is inserted between the fluorescent emitter (BTPE-PI) and the phosphorescent emitter Ir(ppy)$_3$ to confine the singlet excitons and their recombination in the BTPE-PI region. This configuration is expected to harvest both single and triplet excitons.[75] The device emits intense white light ($L_{\max}$ = 17900 cd/m^2) through the simultaneous emission from the primary RGB emitters and shows excellent performance with $\eta_{C,\max}$, $\eta_{P,\max}$ and $\eta_{ext,\max}$ of, 12.3 cd/A, 9.5 lm/W and 7.3%, respectively (Figure S9). The CIE coordinates are calculated to be (0.31, 0.32) at 8 V, which are slightly deviated from the values of the theoretical white point (0.33, 0.33)[74] due to insufficient green and red components in the emission spectrum. To further improve the white color purity, we optimized the device configuration and chose CBP (E_{LUMO} = −2.8 eV) as the buffer layer, whose LUMO energy level is 0.4 eV lower than that of mCP (E_{LUMO} = −2.4 eV). This buffer layer should facilitate more electrons and thus more recombination in the green and red emission layers due to no injection barrier from the buffer layer to the green and red emitting layers (Figure 6B). Thus, another WOLED device with a configuration of ITO/NPB(40 nm)/Ir(btp)$_2$(acac)(6 wt %):CBP(10 nm)/Ir(ppy)$_3$(8 wt %):CBP(4 nm)/CBP(3 nm)/BTPE-PI(5 nm)/TPBi(40 nm)/LiF/Al (Device III) was constructed. The device starts to emit at 3.2 V, showing similar intense white emission with $L_{\max}$, $\eta_{C,\max}$, $\eta_{P,\max}$, and $\eta_{ext,\max}$ of 19200 cd/m^2, 10.7 cd/A, 8.1 lm/W and 6.4%, respectively (Figure 7 and Table 2). Even at 1000 cd/m^2, high η_{C}, η_{P} and η_{ext} values of 9.8 cd/A, 5.3 lm/W and 5.9%, respectively, are still achieved. More importantly, the CIE coordinates of this device exactly match those of the theoretical white point (0.33, 0.33) at 8 V (Figures 5C and 5D). To the best of our knowledge, it is the first WOLED device with intense emission at theoretical white point fabricated from deep blue AIE fluorophore. In addition, the device shows impressive color stability with CIE coordinates of (0.31, 0.32) even at high voltages of 10 V and 12 V (Figure 7A). This suggests that the hole-electron recombination zone is well confined in the emitting layers in a wide range of working voltage. It is noteworthy that all the EL curves in device I, II and III are smooth, thanks to the high stability of the devices at different applied voltages. Thus, the molecular design strategy present here is simple but successful. It makes full use of the intrinsic advantages of both TPE and conventional chromophores to create deep blue AIE luminogens with efficient solid-state emission and prominent thermal stabilities for high performance OLED applications.

CONCLUSION

In summary, a new efficient deep blue AIE luminogen (BTPE-PI) was designed and synthesized through a simple integration of a weakly conjugated AIE luminogen into a conventional chromophore. The resulting luminogen BTPE-PI shows a weak D-A interaction but a typical AIE characteristic and improved solid-state fluorescence quantum yield than its parent molecules. It also enjoys high thermal stability and good carrier injection capability. Non-doped multilayer EL device fabricated from BTPE-PI shows a small roll-off and emits a deep blue emission with high luminance, current efficiency, power efficiency and external quantum efficiency of 20300 cd/m^2, 5.9 cd/A, 5.3 lm/W and 4.4%, respectively. These results are the best for deep blue AIE emitters reported so far. In addition, for the first time, an efficient AIE-based WOLED using BTPE-PI as deep blue emitter was fabricated and realized pure white light with CIE coordinates of (0.33, 0.33). It is anticipated that by following the molecular design strategy present here, many new efficient deep blue AIE luminophores will be rationally designed and synthesized in the future.

AUTHOR INFORMATION

Corresponding Author

*Ben Zhong Tang, E-mail: tangbenz@ust.hk.

Author Contributions

$^{\perp}$Both authors contributed equally to this work.

ACKNOWLEDGMENT

This work was partially supported by the National Basic Research Program of China (973 Program, 2013CB834701), the University Grants Committee of Hong Kong (AoE/P-03/08) the Research Grants Council of Hong Kong (604913, 16301614, 16305014 and N_HKUST1604114), and the Innovation and Technology Commission (ITCPD/17-9). We thank the support of the Guangdong Innovative Research Team Program (201101C0105067115). We thank Professor Kam Sing Wong in Department of Physics in HKUST for the measurement of fluorescence quantum yields of solid powder samples.

ASSOCIATED CONTENT

Supporting Information Available

NMR, MS, UV, PL, CV spectra, and molecular orbital quantum calculation of PI or BTPE-PI, EL performance of WOLED device. This material is available free of charge via the Internet at http://pubs.acs.org.

REFERENCES

(1) Tang, C. W.; Vanslyke, S. A. Organic Electroluminescent Diodes. *Appl. Phys. Lett.* **1987**, *51*, 913–915.

(2) Huang, H.; Fu, Q.; Zhuang, S.; Liu, Y.; Wang, L.; Chen, J.; Ma, D.; Yang, C. Novel Deep Blue OLED Emitters with 1,3,5-Tri(anthracen-10-yl)benzene-Centered Starburst Oligofluorenes. *J. Phys. Chem. C* **2011**, *115*, 4872–4878.

(3) Yang, X.; Zheng, S.; Bottger, R.; Chae, H. S.; Tanaka, T.; Li, S.; Mochizuki, A.; Jabbour, G. E. Efficient Fluorescent Deep-Blue and Hybrid White Emitting Devices Based on Carbazole/Benzimidazole Compound. *J. Phys. Chem. C* **2011**, *115*, 14347–14352.

(4) Zhu, M. R.; Yang, C. L. Blue Fluorescent Emitters: Design Tactics and Applications in Organic Light-Emitting Diodes. *Chem. Soc. Rev.* **2013**, *42*, 4963–4976.

(5) Hung, L. S.; Chen, C. H. Recent Progress of Molecular Organic Electroluminescent Materials and Devices. *Mat. Sci. Eng. R* **2002**, *39*, 143–222.

(6) Xu, H.; Chen, R. F.; Sun, Q.; Lai, W. Y.; Su, Q. Q.; Huang, W.; Liu, X. G. Recent Progress in Metal–Organic Complexes for Optoelectronic Applications. *Chem. Soc. Rev.* **2014**, *43*, 3259–3302.

(7) Jankus, V.; Chiang, C. J.; Dias, F.; Monkman, A. P. Deep Blue Exciplex Organic Light-Emitting Diodes with Enhanced Efficiency; P-type or E-type Triplet Conversion to Singlet Excitons? *Adv. Mater.* **2013**, *25*, 1455–1459.

(8) Chi, Y.; Chou, P. T. Transition-Metal Phosphors with Cyclometalating Ligands: Fundamentals and Applications. *Chem. Soc. Rev.* **2010**, *39*, 638–655.

(9) Chien, C. H.; Chen, C. K.; Hsu, F. M.; Shu, C. F.; Chou, P. T.; Lai, C. H. Multifunctional Deep-Blue Emitter Comprising an Anthracene Core and Terminal Triphenylphosphine Oxide Groups. *Adv. Funct. Mater.* **2009**, *19*, 560–566.

(10) Hu, J. Y.; Pu, Y. J.; Satoh, F.; Kawata, S.; Katagiri, H.; Sasabe, H.; Kido, J. Bisanthracene-Based Donor–Acceptor-Type Light-Emitting Dopants: Highly Efficient Deep-Blue Emission in Organic Light-Emitting Devices. *Adv. Funct. Mater.* **2014**, *24*, 2064–2071.

(11) Figueira-Duarte, T. M.; Del Rosso, P. G.; Trattnig, R.; Sax, S.; List, E. J. W.; Müllen, K. Designed Suppression of Aggregation in Polypyrene: Toward High-Performance Blue-Light-Emitting Diodes. *Adv. Mater.* **2010**, *22*, 990–993.

(12) Hong, Y. N.; Lam, J. W. Y.; Tang, B. Z. Aggregation-Induced Emission. *Chem. Soc. Rev.* **2011**, *40*, 5361–5388.

(13) Birks, J. B. *Photophysics of Aromatic Molecules. Wiley-Interscience, London*. **1970**.

(14) Shimizu, M.; Hiyama, T. Organic Fluorophores Exhibiting Highly Efficient Photoluminescence in the Solid State. *Chem. Asian J.* **2010**, 5, 1516–1531.

(15) Shirota, Y.; Kinoshita, M.; Noda, T.; Okumoto, K.; Ohara, T. A Novel Class of Emitting Amorphous Molecular Materials as Bipolar Radical Formants: 2-{4-[Bis(4-methylphenyl)amino]phenyl}-5-(dimesitylboryl)thiophene and 2-(4-[Bis(9,9-dimethylfluorenyl)amino]phenyl}-5-(dimesitylborly) thiophene. *J. Am. Chem. Soc.* **2000**, *122*, 11021–11022.

(16) Doi, H.; Kinoshita, M.; Okumoto, K.; Shirota, Y. A Novel Class of Emitting Amorphous Molecular Materials with Bipolar Character for Electroluminescence. *Chem. Mater.* **2003**, *15*, 1080–1089.

(17) Lin, S. L.; Chan, L. H.; Lee, R. H.; Yen, M. Y.; Kuo, W. J.; Chen, C. T.; Jeng, R. J. Highly Efficient Carbazole-π-Dimesitylborane Bipolar Fluorophores for Nondoped Blue Organic Light-Emitting Diodes. *Adv. Mater.* **2008**, *20*, 3947–3952.

(18) Xie, Z.; Yang, B.; Li, F.; Cheng, G.; Liu, L.; Yang, G.; Xu, H.; Ye, L.; Hanif, M.; Liu, S.; Ma, D.; Ma, Y. Cross Dipole Stacking in the Crystal of Distyrylbenzene Derivative: The Approach toward High Solid-State Luminescence Efficiency. *J. Am. Chem. Soc.* **2005**, *127*, 14152–14153.

(19) Würthner, F.; Kaiser, T. E.; Saha-Möller, C. R. J-Aggregates: From Serendipitous Discovery to Supramolecular Engineering of Functional Dye Materials. *Angew. Chem. Int. Ed.* **2011**, *50*, 3376–3410.

(20) Kaiser, T. E.; Wang, H.; Stepanenko, V.; Würthner, F. Supramolecular Construction of Fluorescent J-Aggregates Based on Hydrogen-Bonded Perylene Dyes. *Angew. Chem. Int. Ed.* **2007**, *46*, 5541–5544.

(21) Deans, R.; Kim, J.; Machacek, M. R.; Swager, T. M. A Poly (p-phenyleneethynylene) with a Highly Emissive Aggregated Phase. *J. Am. Chem. Soc.* **2000**, *122*, 8565–8566.

(22) Chen, Z. H.; Bouffard, J.; Kooi, S. E.; Swager, T. M. Highly Emissive Iptycene-Fluorene Conjugated Copolymers: Synthesis and Photophysical Properties. *Macromolecules* **2008**, *41*, 6672–6676.

(23) Moorthy, J. N.; Venkatakrishnan, P.; Natarajan, P.; Lin, Z. H.; Chow, T. J. Nondoped Pure-Blue OLEDs Based on Amorphous Phenylenevinylene-Functionalized Twisted Bimesitylenes. *J. Org. Chem.* **2010**, *75*, 2599–2609.

(24) Liu, C.; Li, Y. H.; Li, Y. F.; Yang, C. L.; Wu, H. B.; Qin, J. G.; Cao, Y. Efficient Solution-Processed Deep-Blue Organic Light-Emitting Diodes Based on Multibranched Oligofluorenes with a Phosphine Oxide Center. *Chem. Mater.* **2013**, *25*, 3320–3327.

(25) Sato, T.; Jiang, D. L.; Aida, T. A Blue-Luminescent Dendritic Rod: Poly(phenyleneethynylene) within a Light-Harvesting Dendritic Envelope. *J. Am. Chem. Soc.* **1999**, *121*, 10658–10659.

(26) Langhals, H.; Krotz, O.; Polborn, K.; Mayer, P. A Novel Fluorescent Dye with Strong, Anisotropic Solid-State Fluorescence, Small Stokes Shift, and High Photostability. *Angew. Chem. Int. Ed.* **2005**, *44*, 2427–2428.

(27) Wang, J.; Zhao, Y.; Dou, C.; Sun, H.; Xu, P.; Ye, K.; Zhang, J.; Jiang, S.; Li, F.; Wang, Y. Alkyl and Dendron Substituted Quinacridones: Synthesis, Structures, and Luminescent Properties. *J. Phys. Chem. B* **2007**, *111*, 5082–5089.

(28) Hong, Y. N.; Lam, J. W. Y.; Tang, B. Z. Aggregation-Induced Emission: Phenomenon, Mechanism and Applications. *Chem. Commun.* **2009**, 4332–4353.

(29) Li, K.; Qin, W.; Ding, D.; Tomczak, N.; Geng, J.; Liu, R.; Liu, J.; Zhang, X.; Liu, H.; Liu, B.; Tang, B. Z. Photostable Fluorescent Organic Dots with Aggregation-Induced Emission (AIE Dots) for Noninvasive Long-Term Cell Tracing. *Sci. Rep.* **2013**, *3*, 1150.

(30) Mei, J.; Hong, Y.; Lam, J. W. Y.; Qin, A.; Tang, Y.; Tang, B. Z. Aggregation-Induced Emission: The Whole Is More Brilliant than the Parts. *Adv. Mater.* **2014**, *26*, 5429–5479.

(31) Huang, J.; Yang, X.; Li, X.; Chen, P.; Tang, R.; Li, F.; Lu, P.; Ma, Y.; Wang, L.; Qin, J.; Li, Q.; Li, Z. Bipolar AIE-Active Luminogens Comprised of an Oxadiazole Core and Terminal TPE Moieties as a New Type of Host for Doped Electroluminescence. *Chem. Comm.* **2012**, *48*, 9586–9588.

(32) Du, X.; Qi, J.; Zhang, Z.; Ma, D.; Wang, Z. Y. Efficient Non-doped Near Infrared Organic Light-Emitting Devices Based on Fluorophores with Aggregation-Induced Emission Enhancement. *Chem. Mater.* **2012**, *24*, 2178–2185.

(33) Dong, Y.; Lam, J. W.; Qin, A.; Liu, J.; Li, Z.; Tang, B. Z.; Sun, J.; Kwok, H. S. Aggregation-Induced Emissions of Tetraphenylethene Derivatives and Their Utilities as Chemical Vapor Sensors and in Organic Light-Emitting Diodes. *Appl. Phys. Lett.* **2007**, *91*, 011111.

(34) Luo, J.; Xie Z.; Lam, J. W. Y.; Cheng, L.; Chenm H.; Qiu C.; Kwok, H. S.; Zhan, X.; Liu, Y.; Zhu, D.; Tang, B. Z. Aggregation-Induced Emission of 1-Methyl-1, 2, 3, 4, 5-pentaphenylsilole. *Chem. Commun.* **2001**, 1740–1741.

(35) Huang, J.; Sun, N.; Dong, Y. Q.; Tang, R. L.; Lu, P.; Cai, P.; Li, Q. Q.; Ma, D. G.; Qin, J. G.; Li, Z. Similar or Totally Different: The Control of Conjugation Degree through Minor Structural Modifications, and Deep-Blue Aggregation-Induced Emission Luminogens for Non-Doped OLEDs. *Adv. Funct. Mater.* **2013**, *23*, 2329–2337.

(36) Huang, J.; Jiang, Y. B.; Yang, J.; Tang, R. L.; Xie, N.; Li, Q. Q.; Kwok, H. S.; Tang, B. Z.; Li, Z. Construction of Efficient Blue AIE Emitters with Triphenylamine and TPE Moieties for Non-Doped OLEDs. *J. Mater. Chem. C* **2014**, *2*, 2028–2036.

(37) Yang, Z. Y.; Chi, Z. G.; Yu, T.; Zhang, X. Q.; Chen, M. N.; Xu, B. J.; Liu, S. W.; Zhang, Y.; Xu, J. R. Triphenylethylene Carbazole Derivatives as a New Class of AIE Materials with Strong Blue Light Emission and High Glass Transition Temperature. *J. Mater. Chem.* **2009**, *19*, 5541–5546.

(38) Yang, Z. Y.; Qin, W.; Lam, J. W. Y.; Chen, S. J.; Sung, H. H. Y.; Williams, I. D.; Tang, B. Z. Fluorescent pH Sensor Constructed from a Heteroatom-Containing Luminogen with Tunable AIE and ICT Characteristics. *Chem. Sci.* **2013**, *4*, 3725–3730.

(39) Yuan, Y.; Li, D.; Zhang, X. Q.; Zhao, X. J.; Liu, Y.; Zhang, J. Y.; Wang, Y. Phenanthroimidazole-derivative semiconductors as

functional layer in high performance OLEDs. *New J. Chem.* **2011**, *35*, 1534–1540.

(40) Gao, Z.; Cheng, G.; Shen, F.; Zhang, S.; Zhang, Y.; Lu, P.; Ma, Y. Highly Efficient Deep Blue Light Emitting Devices Based on Triphenylsilane Modified Phenanthro[9, 10-d]imidazole. *Laser Photon. Rev.* **2014**, *8*, L6–L10.

(41) Xing, X.; Zhang, L. P.; Liu, R.; Li, S. Y.; Qu, B.; Chen, Z. J.; Sun, W. F.; Xiao, L. X.; Gong, Q. H. A Deep-Blue Emitter with Electron Transporting Property to Improve Charge Balance for Organic Light-Emitting Device. *ACS Appl. Mater. Interfaces* **2012**, *4*, 2877–2880.

(42) Al-Riyami, L.; Pineda, M. A.; Rzepecka, J.; Huggan, J. K.; Khalaf, A. I.; Suckling, C. J.; Scott, F. J.; Rodgers, D. T.; Harnett, M. M.; Harnett, W. Designing Anti-inflammatory Drugs from Parasitic Worms: a Synthetic Small Molecule Analogue of The Acanthocheilonema Viteae Product ES-62 Prevents Development of Collagen-Induced Arthritis. *J. Med. Chem.* **2013**, *56*, 9982–10002.

(43) Jana, D.; Boxi, S.; Ghorai, B. K. Synthesis of Gem-Tetraphenylethylene Oligomers Utilizing Suzuki Reaction and Their Aggregation Properties. *Dyes and Pigments* **2013,** 99, 740–747.

(44) Wang, S. J.; Oldham, W. J.; Hudack, R. A.; Bazan, G. C. Synthesis, Morphology, and Optical Properties of Tetrahedral Oligo(phenylenevinylene) Materials. *J. Am. Chem. Soc.* **2000**, *122*, 5695–5709.

(45) Duan, X. F.; Zeng, J.; Lü, J. W.; Zhang, Z. B. Insights into the General and Efficient Cross McMurry Reactions between Ketones. *J. Org. Chem.*, **2006**, *71*, 9873–9876.

(46) Zhang, Y.; Lai, S. L.; Tong, Q. X.; Lo, M. F.; Ng, T. W.; Chan, M. Y.; Wen, Z. C.; He, J.; Jeff, K. S.; Tang, X. L.; Liu, W. M.; Ko, C. C.; Wang, P. F.; Lee, C. S. High Efficiency Nondoped Deep-Blue Organic Light Emitting Devices Based on Imidazole-π-Triphenylamine Derivatives. *Chem. Mater.* **2012**, *24*, 61–70.

(47) Grabowski, Z. R.; Rotkiewicz, K.; Rettig, W. Structural Changes Accompanying Intramolecular Electron Transfer: Focus on Twisted Intramolecular Charge-Transfer States and Structures. *Chem. Rev.* **2003**, *103*, 3899–4032.

(48) Wei, B.; Liu, J. Z.; Zhang, Y.; Zhang, J. H.; Peng, H. N.; Fan, H. L.; He, Y. B.; Gao, X. C. Stable, Glassy, and Versatile Binaphthalene Derivatives Capable of Efficient Hole Transport, Hosting, and Deep-Blue Light Emission. *Adv. Funct. Mater.* **2010**, *20*, 2448–2458.

(49) Wang, Z. M.; Lu, P.; Chen, S. M.; Gao, Z.; Shen, F. Z.; Zhang, W. S.; Xu, Y. X.; Kwok, H. S.; Ma, Y. G. Phenanthro[9,10-d]imidazole as a New Building Block for Blue Light Emitting Materials. *J. Mater. Chem.* **2011**, *21*, 5451–5456.

(50) Wu, W. C.; Yeh, H. C.; Chan, L. H.; Chen, C. T. Red Organic Light-Emitting Diodes with a Non-Doping Amorphous Red Emitter. *Adv. Mater.* **2002**, *14*, 1072–1075.

(51) Yeh, H. C.; Yeh, S. J.; Chen, C. T. Readily Synthesised Arylamino Fumaronitrile for Non-Doped Red Organic Light-Emitting Diodes. *Chem. Commun.* **2003**, 2632–2633.

(52) Chang, S. C.; He, G.; Chen, F. C.; Guo, T. F.; Yang, Y. Degradation Mechanism of Phosphorescent-Dye-Doped Polymer Light-Emitting Diodes. *Appl. Phys. Lett.* **2001**, *79*, 2088–2090.

(53) Zhong, G. Y.; Xu, Z.; He, J.; Zhang, S. T.; Zhan, Y. Q.; Wang, X. J.; Xiong, Z. H.; Shi, H. Z.; Ding, X. M.; Huang, W.; Hou, X. Y. Aggregation and Permeation of 4-(Dicyanomethylene)-2-methyl-6-(p-dimethylaminostyryl)-4H-pyran Molecules in Alq. *Appl. Phys. Lett.* **2002**, *81*, 1122–1124.

(54) Gong, J. R.; Wan, L. J.; Lei, S. B.; Bai, C. L.; Zhang, X. H.; Lee, S. T. Direct Evidence of Molecular Aggregation and Degradation Mechanism of Organic Light-Emitting Diodes under Joule Heating: an STM and Photoluminescence Study. *J. Phys. Chem. B* **2005**, *109*, 1675–1682.

(55) Lee, M. T.; Liao, C. H.; Tsai, C. H.; Chen, C. H. Highly Efficient, Deep-Blue Doped Organic Light-Emitting Devices. *Adv. Mater.* **2005**, *17*, 2493–2497.

(56) Wu, K. C.; Ku, P. J.; Lin, C. S.; Shih, H. T.; Wu, F. I.; Huang, M. J.; Lin, J. J.; Chen, I. C.; Cheng, C. H. The Photophysical Properties of Dipyrenylbenzenes and Their Application as Exceedingly Efficient Blue Emitters for Electroluminescent Devices. *Adv. Funct. Mater.* **2008**, *18*, 67–75.

(57) Lee, S. J.; Park, J. S.; Yoon, K. J.; Kim, Y. I.; Jin, S. H.; Kang, S. K.; Gal, Y. S.; Kang, S.; Lee, J. Y.; Kang, J. W.; Lee, S. H.; Park, H. D.; Kim, J. J. High-Efficiency Deep-Blue Light-Emitting Diodes Based on Phenylquinoline/Carbazole-Based Compounds. *Adv. Funct. Mater.* **2008**, *18*, 3922–3930.

(58) Chang, H. W.; Kim, Y. H.; Lee, J.; Hofmann, S.; Lüssem, B.; Müller-Meskamp, L.; Gather, M. C.; Leo, K.; Wu, C. C. Color-Stable, ITO-Free White Organic Light-Emitting Diodes with Enhanced Efficiency Using Solution-Processed Transparent Electrodes and Optical Outcoupling Layers. *Org. Electron.* **2014**, *15*, 1028–1034.

(59) Shim, Y. S.; Hwang, J. H.; Lee, H. J.; Choi, K. B.; Kim, K. N.; Park, C. H.; Jung, S. G.; Park, Y. W.; Ju, B. K. Nanoshuttered OLEDs: Unveiled Invisible Auxiliary Electrode. *Adv. Funct. Mater.* **2014**, *24*, 6414–6421.

(60) Sun, J. W.; Lee, J. H.; Moon, C. K.; Kim, K. H.; Shin, H.; Kim, J. J. A Fluorescent Organic Light-Emitting Diode with 30% External Quantum Efficiency. *Adv. Mater.* **2014**, *26*, 5684–5688.

(61) Wang, Z.; Feng, Y.; Zhang, S.; Gao, Y.; Gao, Z.; Chen, Y.; Zhang, X.; Lu, P.; Yang, B.; Chen, P.; Ma, Y.; Liu, S. Construction of High Efficiency Non-Doped Deep Blue Emitters Based on Phenanthroimidazole: Remarkable Substitution Effects on The Excited State Properties and Device Performance. *Phys. Chem. Chem. Phys.* **2014,** *16*, 20772–20779.

(62) Yuan, Y.; Chen, J. X.; Lu, F.; Tong, Q. X.; Yang, Q. D.; Mo, H.-W.; Ng, T. W.; Wong, F. L.; Guo, Z. Q.; Ye, J.; Chen, Z.; Zhang, X. H.; Lee, C. S., Bipolar Phenanthroimidazole Derivatives Containing Bulky Polyaromatic Hydrocarbons for Nondoped Blue Electroluminescence Devices with High Efficiency and Low Efficiency Roll-Off. *Chem. Mater.* **2013,** *25*, 4957–4965.

(63) Li, W.; Liu, D.; Shen, F.; Ma, D.; Wang, Z.; Feng, T.; Xu, Y.; Yang, B.; Ma, Y. A Twisting Donor-Acceptor Molecule with an Intercrossed Excited State for Highly Efficient, Deep-Blue Electroluminescence. *Adv. Funct. Mater.* **2012,** *22*, 2797–2803.

(64) Liu, C.; Gu, Y.; Fu, Q.; Sun, N.; Zhong, C.; Ma, D.; Qin, J.; Yang, C. Nondoped Deep-Blue Organic Light-Emitting Diodes with Color Stability and Very Low Efficiency Roll-Off: Solution-Processable Small-Molecule Fluorophores by Phosphine Oxide Linkage. *Chem. Eur. J.* **2012,** *18*, 13828–13835.

(65) Thangthong, A. M.; Prachumrak, N.; Namuangruk, S.; Jungsuttiwong, S.; Keawin, T.; Sudyoadsuk, T.; Promarak, V. Synthesis, Properties and Applications of Biphenyl Functionalized 9,9-Bis(4-diphenylaminophenyl)fluorenes as Bifunctional Materials for Organic Electroluminescent Devices. *Eur. J. Org. Chem.* **2012,** *2012*, 5263–5274.

(66) Thangthong, A. M.; Meunmart, D.; Prachumrak, N.; Jungsuttiwong, S.; Keawin, T.; Sudyoadsuk, T.; Promarak, V. Bifunctional Anthracene Derivatives as Non-Doped Blue Emitters and Hole-Transporters for Electroluminescent Devices. *Chem. Comm.* **2011,** *47*, 7122–7124.

(67) Zhang, T.; Liu, D.; Wang, Q.; Wang, R.; Ren, H.; Li, J. Deep-Blue and White Organic Light-Emitting Diodes Based on Novel Fluorene-Cored Derivatives with Naphthylanthracene Endcaps. *J. Mater. Chem.* **2011,** *21*, 12969–12976.

(68) Zhu, M.; Wang, Q.; Gu, Y.; Cao, X.; Zhong, C.; Ma, D.; Qin, J.; Yang, C. Efficient Deep-Blue Emitters Comprised of an Anthracene Core and Terminal Bifunctional Groups for Nondoped Electroluminescence. *J. Mater. Chem.* **2011,** *21,* 6409–6415.

(69) Tao, S.; Zhou, Y.; Lee, C. S.; Zhang, X.; Lee, S. T. High-Efficiency Nondoped Deep-Blue-Emitting Organic Electroluminescent Device. *Chem. Mater.* **2010,** *22*, 2138–2141.

(70) Liao, S. H.; Shiu, J. R.; Liu, S. W.; Yeh, S. J.; Chen, Y. H.; Chen, C. T.; Chow, T. J.; Wu, C. I. Hydroxynaphthyridine-

Derived Group III Metal Chelates: Wide Band Gap and Deep Blue Analogues of Green Alq3 (Tris(8-hydroxyquinolate)aluminum) and Their Versatile Applications for Organic Light-Emitting Diodes. *J. Am. Chem. Soc.* **2009,** *131*, 763–777.

(71) Chen, W. C.; Yuan, Y.; Wu, G. F.; Wei, H. X.; Tang, L.; Tong, Q. X.; Wong, F. L.; Lee, C. S. Staggered Face-to-Face Molecular Stacking as a Strategy for Designing Deep-Blue Electroluminescent Materials with High Carrier Mobility. *Adv. Opt. Mater.* **2014**, *2*, 626–631.

(72) Chen, W. C.; Yuan, Y.; Wu, G. F.; Wei, H. X.; Ye, J.; Chen, M.; Lu, F.; Tong, Q. X.; Wong, F. L.; Lee, C. S. Molecular Modification on Bisphenanthroimidazole Derivative for Deep-Blue Organic Electroluminescent Material with Ambipolar Property and High Performance. *Org. Electronics* **2015**, *17*, 159–166.

(73) Lee, B. M.; Kim, N. H.; Yoon, J. A.; Lee, S. E.; Kim, Y. K.; Kim, W. Y.; Mascher, P. Luminescence Characteristics of Hybrid Dual Emitting Layers in Blue Organic Light-Emitting Diodes by Controlling the Fluorescent Doping Concentration. *J. Lumines.* **2014**, *148*, 72–78.

(74) Ying, L.; Ho, C. L.; Wu, H. B.; Cao, Y.; Wong, W. Y. White Polymer Light-Emitting Devices for Solid-State Lighting: Materials, Devices, and Recent Progress. *Adv. Mater.* **2014**, *26*, 2459–2473.

(75) Schwartz, G.; Reineke, S.; Rosenow, T. C.; Walzer, K.; Leo, K. Triplet Harvesting in Hybrid White Organic Light-Emitting Diodes. *Adv. Funct. Mater.* **2009**, *19*, 1319–1333.

Construction of Efficient Deep Blue AIE Luminogen from Triphenylethene for Non-Doped OLED Applications